ELSEVIER

Journal of Alloys and Compounds 444–445 (2007) 300–304

Journal of ALLOYS AND COMPOUNDS

www.elsevier.com/locate/jallcom

Atomistic study of small helium bubbles in plutonium

B.Y. Ao [a,*], X.L. Wang [a], W.Y. Hu [b], J.Y. Yang [b], J.X. Xia [b]

[a] China Academy of Engineering Physics, P.O. Box 919-71, Mianyang 621900, Sichuan, People's Republic of China
[b] Department of Applied Physics, Hunan University, Changsha 410082, Hunan, People's Republic of China

Received 26 April 2006; received in revised form 31 October 2006; accepted 2 November 2006
Available online 27 December 2006

Abstract

An EAM (embedded atom method) potential is constructed for fcc δ-Pu. MD (molecular dynamics) simulations with the potential are performed to investigate the behavior of small He bubbles in Pu. The simulation results show that He bubble growth can be governed by the mechanism of dislocation-loop punching. The equilibrium structures of the He bubbles with different size are determined. It is clearly shown that dislocation loops are formed around the He bubbles. Moreover, the swelling of computational cells containing He bubbles is predicted.

PACS: 61.72.−y; 61.72.Cc; 61.72.Qq

Keywords: Molecular dynamics; Plutonium; Helium; Crystal defects

1. Introduction

Pu is vulnerable to aging because it is a radioactive element, decaying to U by emitting α particle. The 86 keV ^{235}U recoil traverses the lattice approximately 12 nm and results in the formation of approximately 2300 Frenkel pairs. Although 90% of these Frenkel pairs return to the initial lattice sites with the first 200 ns, the remaining 10% remain in the lattice in the form of free SIA (self-interstitial atoms) and vacancies or SIA or vacancy clusters. On the other side of the decay, a 5 MeV α particle traverses the lattice approximately 10 μm, slowly losing its energy via electronic excitations before coming to rest with the generation of an additional 265 Frenkel pairs. Although the widely used ^{239}Pu has a relatively long half-life of about 24,000 years, its decay rate is still sufficiently high to lead to a significant buildup of He and radiation damage within the metal after several decades [1,2]. As is well known, He and radiation damage in metals can produce macroscopic detrimental effects such as swelling and embrittlement, thus alter the properties of metals and alloys. Beyond all doubt, Pu and its alloys must also be the very typical examples.

Despite some researches regarding He effects and radiation damage in Pu with direct and indirect techniques, many questions remain unsolved [3–7]. In order to obtain further knowledge about the behavior of He in Pu, MD simulations are performed to investigate the problem. However, the discussion on displacement cascades such as defects evolution in Pu is beyond the scope of this paper. In our previous works, the behaviors of He-vacancy clusters and the interactions between points defects and extended defects were studied. In the present paper, we extend our previous work by using the same computational methods to research the behavior of small He bubbles in Pu.

2. Method of calculations

2.1. Molecular dynamics

A complete understanding of the behavior of small He bubble in Pu requires an atomic-level computer simulation. MD simulation is an important tool for understanding materials at atomic level. By using MD simulation, the behaviors of defects in solid materials can be directly probed. The general methods of MD simulation have been discussed in great details by a number of authors; thus, we give here only the specific details of our calculations. In the present MD simulation, the six-value Gear predictor–corrector algorithm and Nosé constant-temperature technique [8], with a time step of 1 fs are employed.

The MD simulations consider a periodic cubic cell of $14a_0 \times 14a_0 \times 14a_0$, where a_0 is the lattice constant of fcc δ-Pu. The simulation cell contains 10,976 Pu lattice sites. Several He atoms are initially placed

* Corresponding author. Tel.: +86 816 362 5457.
E-mail address: aobingyun24@yahoo.com.cn (B.Y. Ao).

0925-8388/$ – see front matter © 2006 Elsevier B.V. All rights reserved.
doi:10.1016/j.jallcom.2006.11.077

in the neighboring interstitial sites. The MD simulations are allowed to run until equilibrium is reached. As illustrated by our previous research, those He atoms can cluster together by self-trapping mechanism. Then more He atoms are added to the He-vacancy cluster and the system is again equilibrated. The simulation temperature is chosen as 300 K.

2.2. The potentials

The success of the MD simulation lies in the choice of the interatomic potentials of Pu–Pu and Pu–He. We have developed our own Pu–Pu EAM potential to reproduce the fcc δ-Pu, and Pu–He Morse pair potential. In the original EAM model, there are two assumptions [9]. First, the atomic electron densities are to be well represented by the spherically averaged free atom densities calculated from Hartree–Fock theory. Second, the host electron density is approximated by a linear superposition of the atomic densities of the constituents. These assumptions are too simple and cannot describe the actual situation well. Baskes modified it to include direct and bonding in the expression of electron density, and applied to variety of cubic materials [10], but the calculations were very complicated. Our group proposed another modified method [11]. With introducing a modified energy term $M(P)$ to the total energy expression to express the energy difference resulting from the electron density difference and to correct the negative Cauchy relation, a new type of modified analytic EAM (MAEAM) has been constructed for almost all typical metals [12–17].

The present MAEAM describes the total energy E_t of any structure as the sum of three terms, a many-body term depending on the local electron density, a two-body term depending on interatomic distances, and a modification term to correct for the assumption of the linear superposition of atomic electron density in the original EAM [14–17]:

$$E_t = \sum_i F(\rho_i) + \frac{1}{2}\sum_{i,j}\phi(r_{ij}) + \sum_i M(P_i) \quad \text{for } i \neq j, \tag{1}$$

where $\phi(r)$ is the effective two-body potential and $F(\rho)$ is the embedding energy. The local electron density ρ_i and its second order P_i are determined by a superposition of individual atomic electron densities $f(r_{ij})$:

$$\rho = \sum_m f(r_m), \tag{2}$$

$$P = \sum_m f^2(r_m), \tag{3}$$

where m is the number of the neighbor atoms. The atomic electron density is described by the function $f(r)$:

$$f(r) = \left(\frac{r_1}{r}\right)^{4.7}\left[\frac{r_{ce}-r}{r_{ce}-r_1}\right]^2, \tag{4}$$

where r_1 is the nearest neighbor atomic equilibrium distance, $f(r)$ is truncated at r_{ce}, $r_{ce} = r_4 + 0.75(r_5 - r_4)$, where r_4 and r_5 are the fourth and fifth neighbor distances for a perfect crystal, respectively.

The energy modification term is empirically taken as

$$M(P) = \alpha\left\{1 - \exp\left[-10^4\left(\ln\left(\frac{P}{P_e}\right)\right)^2\right]\right\}, \tag{5}$$

where P_e is its equilibrium value.

Table 1
The input physical parameters for the δ-Pu MAEAM potential, a is the lattice constant, E_c the cohesive energy, E_{1f} the mono-vacancy formation energy, and C_{11}, C_{12} and C_{44} are the elastic constants

a (nm)	0.464
E_c (eV)	4.2
E_{1f} (eV)	0.9
C_{11} (GPa)	38.0
C_{12} (GPa)	26.0
C_{44}(GPa)	33.0

The embedding functions of $F(\rho)$ take the same forms as those used by Johnson [18]:

$$F(\rho) = -F_0\left[1 - n\left(\ln\frac{\rho}{\rho_e}\right)\right]\left(\frac{\rho}{\rho_e}\right)^n, \tag{6}$$

where F_0 and n are the model parameters and ρ_e is the equilibrium electron density.

A Morse-like pair potential is proposed in the frame of our MAEAM. The proposed pair potential $\phi(r)$ is,

$$\begin{aligned}\phi(r) = {} & k_0 + k_1\exp\left(1 - \frac{r}{r_1}\right) + k_2\exp\left[2\left(1 - \frac{r}{r_1}\right)\right] \\ & + k_3\exp\left[3\left(1 - \frac{r}{r_1}\right)\right] + k_4\exp\left[4\left(1 - \frac{r}{r_1}\right)\right] \\ & + k_{-1}\exp\left(\frac{r_1}{r} - 1\right),\end{aligned} \tag{7}$$

where k_i ($i = -1$, 0, 1, 2, 3 and 4) is the potential parameters. In the present model, the atomic interactions up to the third neighbor distance are considered and $\phi(r)$ is truncated between the third and the fourth neighbor distance, $r_c = r_3 + 0.75(r_4 - r_3)$. At this point, the pair potential and its slope are zero, i.e.

$$\phi(r_c) = 0, \qquad \phi'(r_c) = 0. \tag{8}$$

All the model parameters are determined analytically by fitting the properties of metals, such as lattice constants a, cohesive energy E_c, mono-vacancy formation energy E_{1f}, and elastic constants C_{11}, C_{12}, C_{44}. The input physical parameters for Pu [19–21] are listed in Table 1. Although this potential is for pure Pu, the elastic constants and the mono-vacancy formation energy are taken from a Ga-stabilized Pu δ-alloy (fcc crystal structure). The Pu EAM potential has been proven to be effective to a certain extent to reproduce many properties of Pu, but it cannot reproduce the complicated phase transformations [20,22–25]and cannot reproduce the unusual phonon softening in δ-Pu. In fact, many of these difficulties can be corrected only by the most advanced electronic structure calculation methods, for example, the recently developed dynamics mean field theory (DMFT) has been succeeded in reproducing the unusual phonon softening in δ-Pu [21,26,27]. From the viewpoint of atomic-level computer simulation, the Pu MAEAM potential can be tentatively used to investigate the atomic behavior of defects in Pu.

The He–He potential used is of the Lennard–Jones pair potential [28]:

$$\phi = \phi_0\left[\left(\frac{r_0}{r}\right)^{12} - 2\left(\frac{r_0}{r}\right)^6\right], \tag{9}$$

where ϕ_0 and r_0 are the potential parameters. The He–He potential has been widely used to study He effects in solid materials.

For the Pu–He cross potential, there is no experimental data at all with which to fit the potential. As is well known, He atom has a filled-shell electronic configuration and is thus likely to interact with other

atoms in a simpler way than do metal atoms, in other words, the electronic effects of He–metals interactions may be negligible. For this reason, the Pu–He cross potential was modelled as Morse pair potential:

$$\phi = \phi_0 \left[\exp\left(-2\alpha\left(\frac{r}{r_0} - 1\right)\right) - 2\exp\left(-\alpha\left(\frac{r}{r_0} - 1\right)\right)\right], \quad (10)$$

where ϕ_0, r_0 and α are the potential parameters. In order to determine the potential parameters, we try to compare Pu with other fcc metals (such as Al, Pd and Ni) whose interaction potentials with He were developed by using first-principles calculations [29]. We have obtained the potential parameters by choosing from a variety of values of ϕ_0, r_0 and α. Although the fidelity of the potential parameters is limited, the Pu—He cross potential is qualitatively feasible for modelling the behavior of He atoms in Pu. Furthermore, the selected potential parameters are in accordance with the Pu–He dimer potential developed by using *ab initio* calculations [30].

3. Results and discussion

We have found that five He atoms in Pu can cluster by self-trapping mechanism, creating a Frenkel pair and a deeply bound cluster. The introduction of further interstitial He atoms produces many more Frenkel pairs. After reaching a certain He-vacancy size, the punching out of dislocation loop is energetically more favorable. In fact, the punching out of dislocation can be viewed as the extension of He self-trapping [31,32].

The three-dimensional structure of a bubble containing 216 He atoms is shown in Fig. 1. The initial configuration of interstitial He atoms is very sparse. After MD relaxation, most of the He atoms cluster together forming a compact He bubble. Only a few of He atoms are apart from the He bubble, forming some substitutional He atoms (replacement of Pu atom with He atom) and some very small He-vacancy clusters. The dynamics process shows that He bubble forms at the beginning of MD simulation, which implies that initial configuration of interstitial He atoms is very instable and the equilibrium configuration of He bubble is relatively stable. The projection of the simulation cell containing a bubble of 216 He atoms is shown in Fig. 2. The initial configuration of simulation cell is perfect fcc lattice. During the process of He bubble growth, many Pu atoms around He bubble are pushed off the normal lattice sites, finally, those Pu atoms form a distinct dislocation loop, i.e. the rectangle of self-interstitial Pu atoms around He bubble in the figure. The most remarkable property of the dislocation loop is that all the Pu atoms inside the dislocation loop still stay at the normal lattice sites while the Pu atoms of the dislocation is disorder, as shown in Fig. 3 where He bubble is not displayed. When He bubble is removed and the cell is performed MD simulation again, most of those Pu atoms of dislocation loop approximately come back to their normal lattice sites and only a few of Pu atoms form crowded interstitial atoms.

As discussed by many researchers, He bubble in metals may show a packing structure mainly due to crystal stresses. However, the structure of He bubble strongly depends on He atomic density (He-vacancy atomic ratio). We have found that the configuration of He atoms in relatively small He-vacancy cluster shows fcc-like packing. As for He bubble with high He atomic

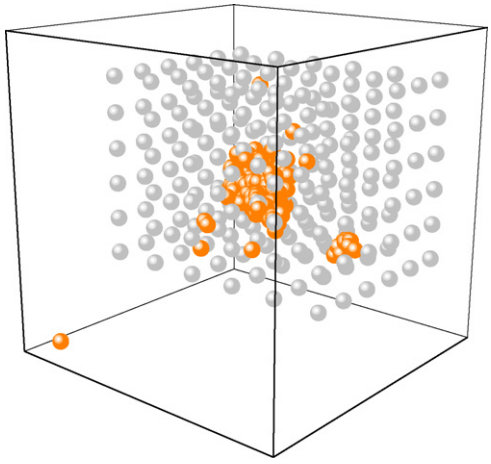

Fig. 1. 3D configuration of He atoms before and after bubble formation. The light gray balls represent the initial sites of He atoms, while the equilibrium sites of these He atoms are indicated by orange balls.

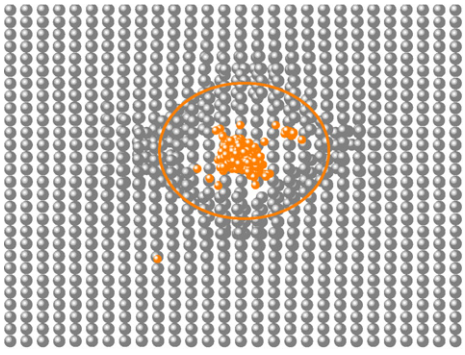

Fig. 2. Projection of simulation cell containing a bubble of 216 He atoms. Pu and He atoms are denoted by gray and orange balls, respectively. The dislocation loop is indicated by orange circle.

density, He atoms do not show perfect fcc packing, but He bubble shows a compact ellipsoidal structure, as revealed in Fig. 4.

The swelling induced by He bubble growth is shown in Fig. 5 as a function of He atomic concentration. The swelling is defined by $S = (V - V_0)/V_0$, where V is the equilibrium volume of the relaxed simulation cell containing a bubble and V_0 is the initial volume in the absence of bubble. For low He concentration, swelling increases linearly with increasing He concentration. However, swelling does not increase linearly with

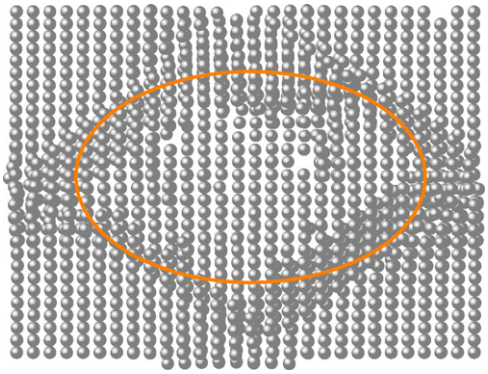

Fig. 3. Projection of simulation cell containing a large dislocation loop. He atoms are not shown in the figure.

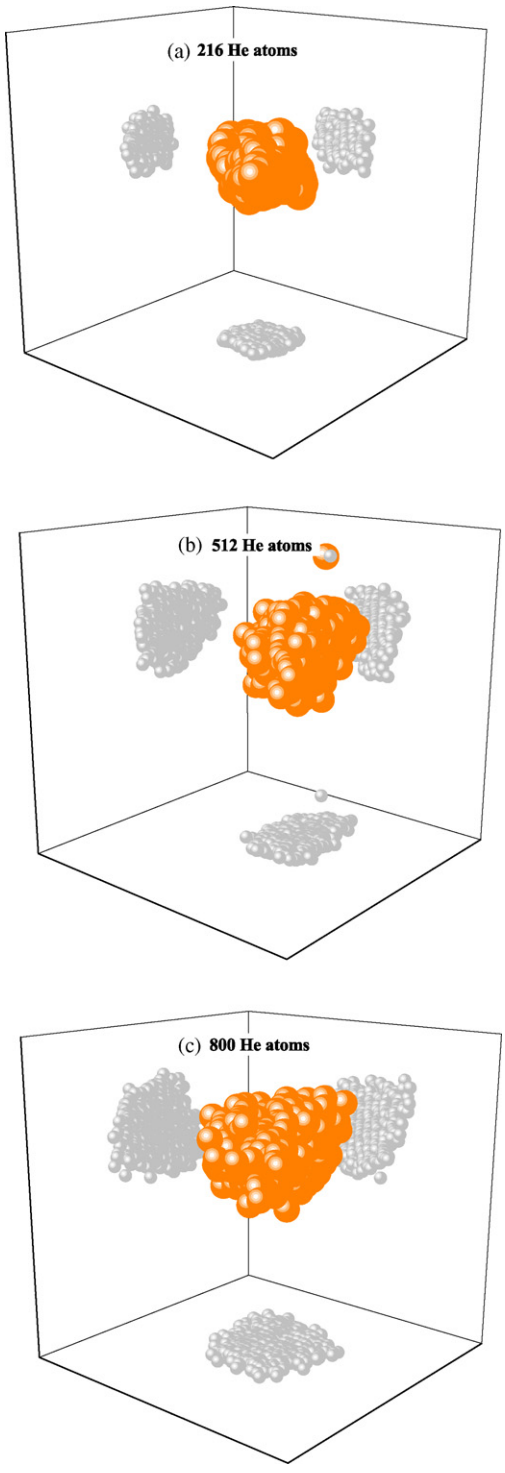

Fig. 4. 3D configurations of He bubbles and their projections on three planes. The orange and light gray balls designate He atoms and their projections, respectively. (a) 216 He atoms, (b) 512 He atoms and (c) 800 He atoms.

high He concentration. As is well known, one of very important macroscopical effects of He in metals is swelling due to He bubble formation and growth. As shown in the figure, the swelling induced by He bubble in δ-Pu is very small. For δ-Pu, the cumulative rate of He production is about 40 atomic parts per million per year (appm/year). Even after 40 years of self-radiation aging, the swelling is still less than 1. From the calculated results, we

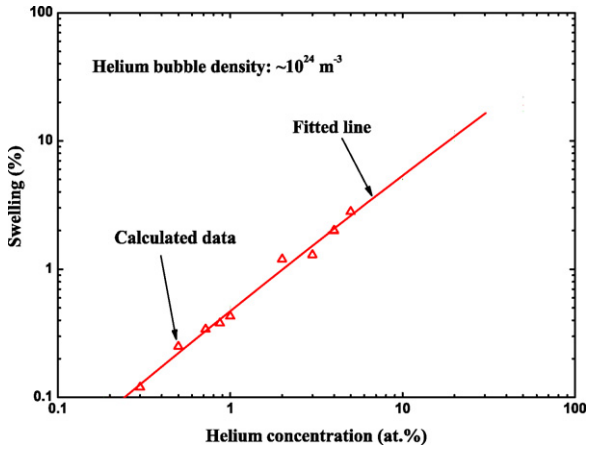

Fig. 5. Calculated results for swelling of Pu containing He bubble.

can infer that swelling due to He bubble is less serious than other possible mechanism, such as void swelling. In fact, our previous MD results have indicated that grain boundary and dislocation can act as sinks and sources of self-interstitial atoms, which may be a reason for the swelling of Pu after a period of self-radiation aging because of the higher concentration of vacancy in the bulk.

4. Conclusion

A computational framework based on MD simulations and EAM potential to investigate the behavior of small He bubble in δ-Pu has been presented. He bubble formation and growth can be interpreted by dislocation loop punching, which is a very common phenomenon in metals. The results indicate that formation of dislocation loop gives rise to an energetically more favorable zone for He bubble formation and growth. In addition, the swelling induced by He bubble may be less serious than other possible mechanism, such as void swelling. However, as the extraordinary complexity of Pu and its self-radiation aging effects, more works on the behavior of He bubble are under way.

Acknowledgements

This work was supported by the Science and Technology Foundation of China Academy of Engineering Physics (No. 20040546), and High Performance Computing Center of Hunan University.

References

[1] W.G. Wolfer, in: N.G. Cooper (Ed.), Challenges in Plutonium Science, Los Alamos Science, vol. 26, Los Alamos Laboratory, 2000, p. 274.
[2] B.D. Wirth, A.J. Schwartz, M.J. Fluss, M.J. Caturla, M.A. Wall, W.G. Wolfer, MRS Bull. 26 (2000) 679.
[3] D. Dooley, B. Martinez, D. Olson, D. Olivas, R. Ronquillo, T. Rising, K.K.S. Pillay, K.C. Kim (Eds.), Plutonium Future—The Science, American Institute of Physics, 2000, p. 428.
[4] C. Ronchi, J.P. Hiernaut, J. Nucl. Mater. 35 (2004) 1.
[5] T.G. Zocco, in: N.G., Cooper (Ed.), Challenges in Plutonium Science, Los Alamos Science, vol. 26, Los Alamos Laboratory, 2000, p. 286.
[6] P.G. Klemens, B. Cort, J. Alloys Compd. 252 (1997) 157.

[7] D.C. Swift, L.G. Mallinson (Eds.), Aging Studies and Lifetime Extension of Materials, Kluwer Academic, New York, 2001, p. 375.
[8] S. Nosé, Prog. Theor. Phys. Suppl. 103 (1991) 1.
[9] M.S. Daw, M.I. Baskes, Phys. Rev. B 29 (1984) 6443.
[10] M.I. Baskes, Phys. Rev. B 46 (1992) 2727.
[11] Y. Ouyang, B. Zhang, S. Liao, Z. Jin, Z. Phys. B 101 (1996) 161.
[12] H. Deng, W.Y. Hu, X. Shu, B. Zhang, Surf. Sci. 543 (2003) 95.
[13] J. Yang, W.Y. Hu, H. Deng, D. Zhao, Surf. Sci. 572 (2004) 439.
[14] W.Y. Hu, B. Zhang, B. Huang, F. Gao, D.J. Bacon, J. Phys.: Conden. Matter 13 (2001) 1193.
[15] W.Y. Hu, H. Deng, M. Fukumoto, Euro. Phys. J. B 34 (2003) 429.
[16] W.Y. Hu, X. Shu, B. Zhang, Comput. Mater. Sci. 23 (2002) 175.
[17] W.Y. Hu, M. Fukumoto, Model. Simul. Mater. Sci. Eng. 10 (2002) 707.
[18] R.A. Johnson, Phys. Rev. B 41 (1990) 9717.
[19] P. Pochet, Nucl. Instrum. Meth. Phys. Res. B 202 (2003) 82.
[20] M.I. Baskes, Phys. Rev. B 62 (2000) 15532.
[21] X. Dai, S.Y. Savrasov, G. Kotliar, A. Migliori, H. Ledbetter, E. Abrahams, Science 300 (2003) 953.
[22] F.J. Cherne, M.I. Baskes, B.L. Holian, Phys. Rev. B 67 (2003) 092104.
[23] S.M. Valone, M.I. Baskes, M. Stan, T.E. Mitchell, A.C. Lawson, K.E. Sickafus, J. Nucl. Mater. 324 (2004) 41.
[24] M.J. Fluss, B.D. Wirth, M. Wall, T.E. Felter, M.J. Caturla, A. Kubota, T. Diaz de la Rubia, J. Alloys Compd. 368 (2004) 62.
[25] M.I. Baskes, K. Muralidharan, M. Stan, S.M. Valone, F.J. Cherne, JOM 9 (2003) 41.
[26] J. Wong, M. Krisch, D.L. Farber, F. Occelli, A.J. Schwartz, T.C. Chiang, M. Wall, C. Boro, R. Xu, Science 301 (2003) 1078.
[27] R.J. McQueeney, A.C. Lawson, A. Migliori, T.M. Kelley, B. Fultz, M. Ramos, B. Martinez, J.C. Lashley, S.C. Vogel, Phys. Rev. Lett. 92 (2004) 146401.
[28] R.A. Johnson, J. Phys. F: Met. Phys. 3 (1973) 295.
[29] M.I. Baskes, C.F. Melius, Phys. Rev. B 20 (1979) 3197.
[30] S.M. Valone, M.I. Baskes, R.L. Martin, LA-UR-02-1958, Los Alamos National Laboratory, 2002.
[31] W.G. Wolfer, Phil. Mag. A 58 (1988) 285.
[32] J.B. Adams, W.G. Wolfer, S.M. Foiles, C.M. Rohlfing, C.D. van Siclen, S.E. Donnelly, J.H. Evans (Eds.), Fundamentals Aspects of Inert Gases in Solids, Plenum Press, New York, 1991, p. 1.